Research in Pharmaceutical Sciences, October 2022; 17(5): 482-492
Received: 12-02-2022
Peer Reviewed: 15-03-2022
Revised: 08-05-2022
Accepted: 09-07-2022
Published: 08-09-2022

School of Pharmacy & Pharmaceutical Sciences
Isfahan University of Medical Sciences

Original Article

Design and synthesis of some novel triazine-tyrosine hybrids as potential agents for the treatment of multiple sclerosis

Sajjad Saeidi[1], Parvin Asadi[1,2], Farshid Hassanzadeh[1], Mehdi Aliomrani[2,3], and Ghadam Ali Khodarahmi[1,2,*]

[1]*Department of Medicinal Chemistry, School of Pharmacy and Pharmaceutical Sciences, Isfahan University of Medical Sciences, Isfahan, I.R. Iran.*
[2]*Isfahan Pharmaceutical Sciences Research Center, School of Pharmacy and Pharmaceutical Science, Isfahan University of Medical Sciences, Isfahan, I.R. Iran.*
[3]*Department of Pharmacology and Toxicology, School of Pharmacy and Pharmaceutical Science, Isfahan University of Medical Sciences, Isfahan, I.R. Iran.*

Abstract

Background and purpose: One of the most noteworthy methods to slow down multiple sclerosis (MS) progress is a decrease of lymphocyte cells *via* S1P1 receptor modulating. Here, a series of S1P1 receptor modulators were designed and investigated for their ability to decrease lymphocytes in a rat model.
Experimental approach: Molecular docking was performed to compare the binding mode of desired compounds **5a-f** with fingolimod to the active site of the S1P1 receptor, theoretically. To prepare desired compounds, **5a-f**, cyanuric chloride was reacted with different amines, **a-f,** which then converted to **4a-f** compounds through reaction with N-boc-Tyr-OMe ester. Finally, deprotection of the carboxyl and amino groups was carried out to obtain **5a-f** as final products. Lymphocyte counting in the rat model was carried out using flow cytometry to evaluate the efficacy of the suggested compounds**.**
Findings / Results: All compounds exhibited lower binding energy than fingolimod. Compound **5e** with ΔG = -8.10 kcal/mol was the best compound. The structure of the compounds was confirmed spectroscopically. The *in vivo* study proved that compounds **5b** and **5a** decreased the lymphocytes level at 0.3 and 3 mg/kg, respectively.
Conclusion and implications: The desired compounds were well fitted in the receptor active site following molecular docking studies. The results of lymphocyte count revealed that compounds **5a** and **5b** with propyl and ethyl substitutes showed the maximum activity *in vivo*. Finally, the results of the present project can be used for forthcoming investigations towards the design and synthesis of novel potential agents for MS treatment.

Keywords: Lymphocyte counts; Molecular docking; Multiple sclerosis; S1P1R modulator.

INTRODUCTION

Multiple sclerosis (MS), the most common immune-mediated disorder (1), is an unpredictable, chronic autoimmune, inflammatory neurological disorder affecting the central nervous system (2,3). MS interrupts the communication between the brain and body by attacking the myelin covering nerve fibers (4). It is supposed that environmental and genetic factors are contributors to the risk of MS; however, its etiology is still unidentified.

*Corresponding author: Gh.A. Khodarahmi
Tel: +98-3137927095, Fax: +98-3136680011
Email: khodarahmi@pharm.mui.ac.ir

Sphingosine-1-phosphate (S1P), a signaling lipid, has significant regulatory roles in the body, such as proliferation, survival and migration of cells, inflammation, vascular permeability, and immune response through five subfamilies of the receptors (5-9). S1P1, as a first subtype of the S1P receptor (S1PR), has a key role in lymphocyte trafficking regulation, which makes it a therapeutic target for the treatment of MS.

Access this article online

Website: http://rps.mui.ac.ir

DOI: 10.4103/1735-5362.355208

This subtype (S1P1) is expressed on the surfaces of different cells like neural cells, lymphocytes, and endothelial cells (10,11).

Fingolimod (FTY720), a compound that interacts with S1PR, was approved in 2010 for the treatment of MS (12). Fingolimod slows down the progression of disability and prevents episodes of signs of relapsing-remitting MS. Fingolimod and sphingosine are structurally analogous, but *in vivo* phosphorylation must happen for activation of fingolimod to produce fingolimod-phosphate (fingolimod-P) (13). Then fingolimod-P, as an S1PR modulator, competes with S1P for the receptor and exerts its therapeutic effects (14). However, hypertension, headache, bradycardia, and atrioventricular block are the most common side effects of fingolimod (11).

According to the previous studies, all S1P1 modulators have three main parts including (1) a polar head group, (2) a linker which commonly consists of a heterocycle or aromatic ring, and (3) a nonpolar chain located in the tail of the molecules (Scheme 1) (15-18). The structure-activity relationship (SAR) studies indicate that minor changes to the linker core could lead to selective, potent, and novel new S1P1 modulators (17). For example, the study by Chen *et al.* showed that different isoforms of oxadiazole ring as a core could demonstrate a 10-fold increase in S1P1 activation than fingolimod (18).

Considering the perivenous studies (15-18), our aim was the development of structurally novel S1P1 modulators based on the s-triazine ring and tyrosine structure with potential use as a therapeutic agent against MS. To this end, a series of compounds containing tyrosine as a polar head group, triazine moiety as a linker, and aliphatic amine as a lipophilic tail have been designed (Scheme 1). Subsequently, using the crystallographic structure of hS1P1R, docking studies have been performed to identify possible interactions of derivatives with this receptor, and these compounds were then synthesized. After confirming the purity and identity of the synthesized compounds, the efficacy of the desired compounds was evaluated through lymphocyte counting in a rat model using flow cytometry.

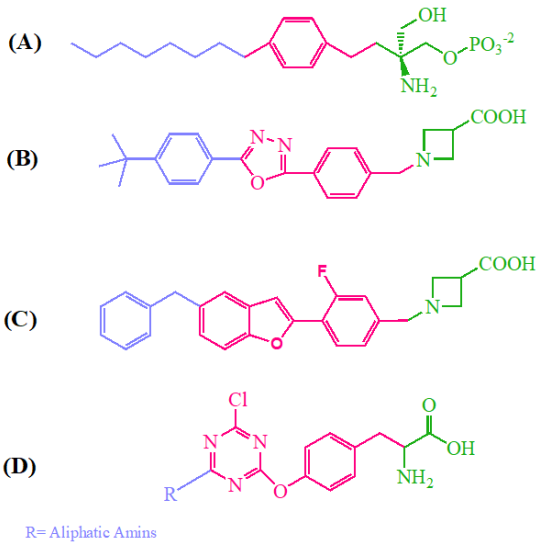

Scheme 1. Design of the hybrid compounds based on the fingolimod and S1P1 modulator structures; (A) fingolimod structure, (B and C) selective S1P1 modulators, and (D) suggested compounds. The purple color represents the lipophilic tail, pink represents the core, and green represents the head group. S1P1, Sphingosine-1-phosphate first subtype.

MATERIALS AND METHODS

All chemicals and reagents were obtained commercially and used without any purification. Reactions were followed by thin-layer chromatography (TLC Silica gel 60 F_{254} pre-coated plates, E. Merck, Germany), and spots were detected by CAMAG UV Cabinet 4 instrument at λ 254 nm. Melting points were measured by an electrothermal melting point apparatus (Electrothermal 9200, USA). Infrared (IR) spectra were recorded on a Rey light WQF-510 IR/Perkin-Elmer1420 Ratio Recording Infrared instrument (USA). The compounds were dissolved in deuterated dimethyl sulfoxide (DMSO-d_6) for proton nuclear magnetic resonance (^{1}H NMR), and the NMR apparatus was Bruker-Ultrashield 400 MHz (USA). Chemical shifts are reported as δ (parts per million, ppm) from tetramethylsilane (TMS) as the internal standard.

In silico procedure

The molecular docking study of six designed compounds **5a-5f** with an S1P1 binding pocket was evaluated by employing protein-ligand docking (19). The RCSB Protein Data Bank (https://www.rcsb.org/) was used to obtain the

crystallography file of the S1P1 protein (PDB ID: 5A86). Co-crystal ligand (fingolimod) and all of the irrelevant compartments were deleted using Discovery Studio Visualizer 4.5 (BIOVIA, San Diego, CA, USA) (20). By using AutoDockTools 1.5.6 (ADT), polar hydrogen and Kollman charges were inserted and a PDBQT file of the protein was generated. The structure of the ligands (**5a-5f**) was drawn and optimized by PM3 semi-empirical force field using Hyperchem software (Version 8Hyperchem, Hypercube, Inc., and Auto Desk, Inc. (21). For the preparation of ligands (**5a-5f**) for docking, Gasteiger charges and polar hydrogens were added and non-polar hydrogens merged. In all docking procedures, a grid box with 70 × 70 × 70 dimensions and 0.375 Å spacing was applied. The center of the grid box was assigned (27.366, 12.163, and 28.710) according to the centroid of the co-crystal ligand. AutoDock 4.2 was used for each docking procedure (22,23) with 50 runs without changing the defaults of the program, such as search and docking parameters. To validate the procedure, the co-crystal ligand was extracted and re-docked into the protein using the same parameters of docking for designed compounds. All graphical representations of the interactions were produced using PyMOL Molecular Graphics System (24).

Synthesis of compounds

The desired compounds were prepared according to the three following steps:

Step 1: cyanuric chloride 1 (4.3 mmol) was dissolved in acetone (5 mL) in an ice bath. After that, appropriate amine a-f (4.3 mmol) was added dropwise for 10 min. The mixture was stirred at room temperature for 3 h and the progress of the reaction was checked using TLC. After completion of the reaction, the mixture was poured on crushed ice and a white precipitate was obtained. The precipitate was filtered and recrystallized from an ethanol/water (100/1 mL) mixture (24-27).

Step 2: a mixture of **2a-2f** (5 mmol), protected tyrosine **3** (5 mmol), potassium carbonate (7 mmol), and dimethylformamide (5 mL) was stirred at 10-25 °C for 24 h. After completion of the reaction by TLC, the reaction mixture was poured on crushed ice, filtered, washed with water, and recrystallized from the ethanol/water mixture to give compounds **4a-4f** (Table 1).

Table 1. The structure of compounds **4a-4f**.

Compound	Structure
4a	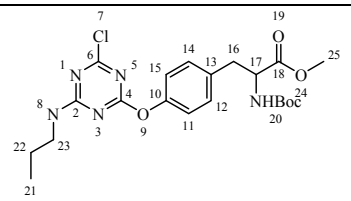
4b	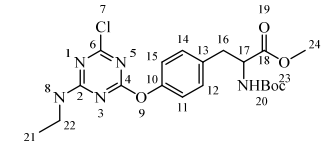
4c	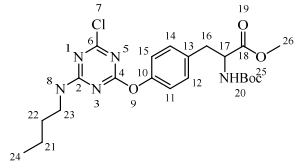
4d	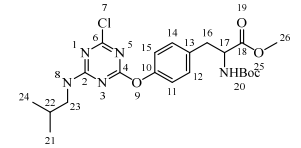
4e	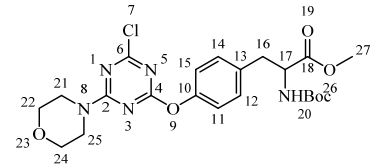
4f	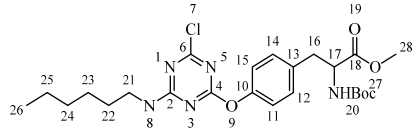

Step 3: in this step, **4a-4f** (0.1 g), was deprotected by dissolving in dioxane and then HCL (2 mL, 7N) and stirred at room temperature for 24 h. After that, the mixture was concentrated and washed with diethyl ether to produce the final products.

In vivo study (counting lymphocyte cells)

In this study, 6-8-week-old male Wistar rats (160-180 mg) were used. The rats were housed at 22 ± 5 °C on a 12/12-h light/dark cycle and kept for three days to get used to the environment with free access to water and food. The animal experimental procedures and protocols were accepted by the Isfahan University of Medical Sciences, Ethics Committee for Laboratory AnimalsEthical No. IR.MUI.RESEARCH.REC.1398.198). These

rats were intraperitoneally dosed with either vehicle control (normal saline and DMSO) or fingolimod and the proposed compounds **5a-5f** (0.3, 1, and 3 mg/kg/day). After 24 h, the rats were anesthetized with the help of an anesthetic, and then retro-orbital blood sampling was performed. The blood samples were evaluated by flow cytometry to count lymphocyte cells.

Statistical analysis

Repeated measure one-way ANOVA was performed in Graphpad Prism software to compare the statistical alterations among groups, and followed up with Tukey post hoc tests. *P*-values ≤ 0.05 were considered significant. Data are presented as mean ± SD.

Table 2. binding energy (ΔG), hydrophobic and H-bonding interactions of proposed compounds and fingolimod in the sphingosine-1-phosphate first subtype active site.

Compounds	Structures	ΔG (kcal/mol)	H-bonding interactions	Hydrophobic interactions
Fingolimod	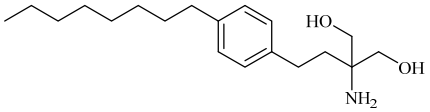	-6.32	SER208 LYS210	HIS242 LEU239 MET243
5a	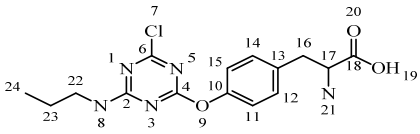	-7.10	LEU209 HIS407 ARG410	PHE288 MET243 VAL211 TRP299
5b	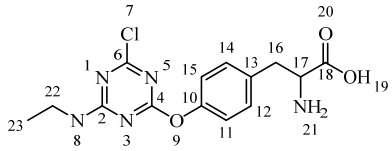	-6.72	LYS210 SER208 GLN285 MET243 SER247	TYR306 VAL211
5c	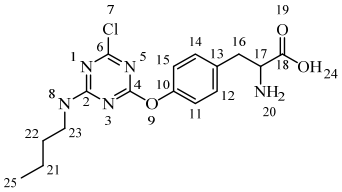	-7.01	SER205 LEU209 HIS407 ARG410	MET243 VAL211 HIS327 TRP299 PHE288
5d	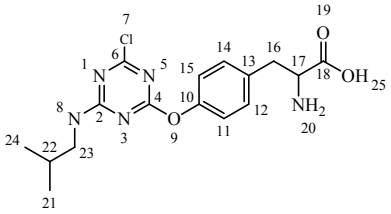	-7.59	SER208 HIS407 ARG410	VAL211 MET243 TPR299 MET246 PHE288 TRP299
5e	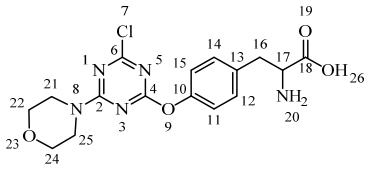	-8.10	LEU209 SER208 HIS 407 ARG410	VAL211 MET243 TRP299 PHE288
5f	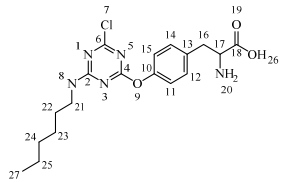	-7.55	LEU209 SER208 HIS 407 ARG410	MET243 VAL211 LEU209 MET323 HIS437 PHE288 TRP299

RESULTS

Molecular docking study

The free binding energies (ΔG), H-bonding, and hydrophobic interactions of the compounds with the binding pocket of S1P1 are depicted in Table 2. Validation of docking procedure was performed by redocking of cocrystal ligand and measurement of root mean square deviation (RMSD). The RMSD value for the re-docking step was 1.3 Å.

Synthesis of compounds

According to Scheme 2, the preparation of compounds included three steps.

Characterization of synthesized compounds

4,6-dichloro-N-propyl-1,3,5-triazin-2-amine (**2a**)

Yield: 85%, white powder, melting point (MP): 145 °C, lit MP: 146 °C (25). Fourier-transform infrared spectroscopy (FT-IR, KBr, cm^{-1}) ν: 3276 (NH), 2970 (CH aliphatic), 1626 (C=N), 1318 (CN), 812 (CCl).

4,6-dichloro-N-ethyl-1,3,5-triazin-2-amine (**2b**)

Yield: 80%, white powder, MP: 109 °C, lit MP: 110 °C (26), FT-IR (KBr, cm^{-1}) ν: 3274 (NH), 2998 (CH aliphatic), 1556 (C=N), 1318 (CN), 834 (CCl).

N-butyl-4,6-dichloro-1,3,5-triazin-2-amine (**2c**)

Yield: 80%, white powder, MP: 49 °C, lit MP: 50 °C (27), FT-IR (KBr, cm^{-1}) ν: 3269 (NH), 2948 (CH aliphatic), 1622 (C=N), 1322 (CN), 813 (CCl).

4,6-dichloro-N-isobutyl-1,3,5-triazin-2-amine (**2d**)

Yield: 85%, white powder, MP: 93 °C, lit MP: 93 °C (27), FT-IR (KBr, cm^{-1}) ν: 3273(NH), 2963 (CH aliphatic), 1626 (C=N), 1321 (CN), 839 (CCl).

4-(4,6-dichloro-1,3,5-triazin-2-yl) morpholine (**2e**)

Yield: 90%, white powder, MP: 127 °C, lit MP:127 °C (26), FT-IR (KBr, cm^{-1}) ν: 2974 (CH aliphatic), 1582 (C=N), 1336 (C-O), 1296 (C-N), 821 (CCl).

4,6-dichloro-N-hexyl-1,3,5-triazin-2-amine (**2f**)

Yield: 70%, white powder, MP: 57 °C, lit MP: 56 °C (28). FT-IR (KBr, cm^{-1}) ν: 3275 (NH), 2939 (CH aliphatic), 1631 (C=N), 1322(CN), 819 (CCl).

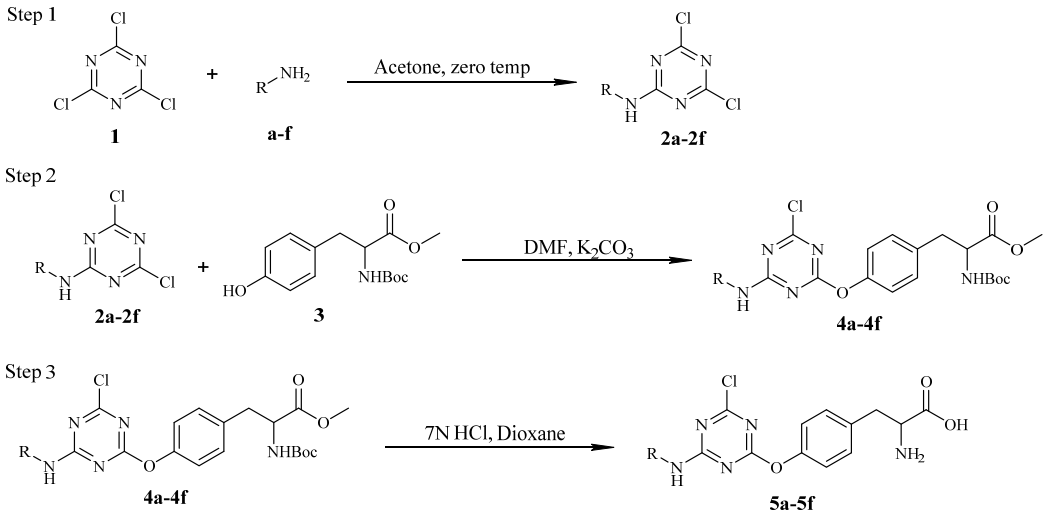

Scheme 2. General procedure for the synthesis of compounds **5a-5f.** DMF**,** Dimethylformamide.

Methyl 2-((tert-butoxycarbonyl)amino)-3-(4-((4-chloro-6-(propylamino)-1,3,5-triazin-2-yl)oxy) phenyl)propanoate (**4a**)

Yield: 75%, white powder, MP: 100 °C, IR (KBr, cm^{-1}) ν: 3365 (NH), 2980 (CH aliphatic), 1716 (C=O), 1586 (CC aromatic), 1291 (C-N), 1190 (C-O), 789 (CCl). ^{1}H NMR (400 MHz, DMSO-d_6) δ: 0.79 (t, 3H, *J* = 3 Hz, H-C^{21}), 1.20 (m, 2H, H-C^{22}), 1.43 (s, 9H, Boc), 2.97 (d, 2H, *J* = 4.1 Hz, H-C^{16}), 3.64 (s, 3H, H-C^{25}), 3.83 (m, 2H, H-C^{23}), 3.85 (br, 1H, H-N^8), 4.18 (m, 1H, H-C^{17}), 5.2 (br, H, H-N^{20}), 7.16 (d, 2H, *J* = 7.2 Hz, H-C^{12}, H-C^{14}), 7.31 (d, 2H, *J* = 7.2 Hz, H-C^{11}, H-C^{15})

Methyl 2-((tert-butoxycarbonyl)amino)-3-(4-((4-chloro-6-(ethylamino)-1,3,5-triazin-2-yl) oxy) phenyl)propanoate (**4b**)

Yield: 65%, white powder, MP: 79 °C, IR (KBr, cm^{-1}) ν: 3417 (NH), 2987 (CH aliphatic), 1734 (C=O), 1612 (C=N), 1573 (CC aromatic), 1299 (CN), 1293 (C-O), 777 (CCl). ^{1}H NMR (400 MHz, DMSO-d_6) δ: 0.70 (t, 3H, H-C^{21}), 1.40 (s, 9H, Boc), 2.98 (d, 2H, H-C^{16}), 3.81 (s, 3H, H-C^{24}), 3.81 (m, 2H, H-C^{22}), 3.90 (br, H, H-N^8), 4.21 (m, H, H-C^{17}), 4.92 (br, H, H-N^{20}), 7.10 (d, 2H, *J* = 7.5 Hz H-C^{12}, H-C^{14}), 7.42 (d, 2H, *J* = 7.2 Hz, H-C^{11}, H-C^{15}).

Methyl 2-((tert-butoxycarbonyl)amino)-3-(4-((4-(butylamino)-6-chloro-1,3,5-triazin-2-yl) oxy) phenyl)propanoate (**4c**)

Yield: 85%, white powder, MP: 81 °C, IR (KBr, cm^{-1}) ν: 3357 (NH), 2961 (CH aliphatic), 1727 (C=O), 1575 (C=N), 1540 (CC aromatic), 1295 (C-N), 1211 (C-O), 709 (CCl). ^{1}H NMR (400 MHz, DMSO-d_6) δ: 0.79 (t, 3H, *J* = 3 Hz, H-C^{24}), 1.20 (m, 4H, H-C^{21}, H-C^{22}), 1.40 (s, 9H, Boc), 2.99 (d, 2H, *J* = 4.1 Hz, H-C^{16}), 3.04 (q, 2H, *J* = 5.4 Hz, H-C^{23}), 3.09 (s, 3H, H-C^{26}), 4.12 (br, H, H-N^8), 4.18 (m, H, H-C^{17}), 5.2 (br, H, H-N^{20}), 7.16 (d, 2H, *J* = 7.2 Hz, H-C^{12}, H-C^{14}), 7.32 (d, 2H, *J* = 7.2 Hz, H-C^{11}, H-C^{15}).

Methyl 2-((tert-butoxycarbonyl)amino)-3-(4-((4-chloro-6-(isobutylamino)-1,3,5-triazin-2-yl)oxy) phenyl)propanoate (**4d**)

Yield: 70%, white powder, MP: 95 °C, IR (KBr, cm^{-1}) ν: 3268 (NH), 2967 (CH aliphatic), 1728 (C=O), 1624 (C=N), 1570 (CC aromatic), 1352 (C-N), 1232 (C-O), 701 (CCl). ^{1}H NMR (400 MHz, DMSO-d_6) δ: 0.88 (d, 6H, *J* = 4 Hz, H-C^{21}, H-C^{24}), 1.33 (s, 9H, Boc), 1.74 (m, H, H-C^{22}), 2.89 (d, 2H, *J* = 4.16 Hz, H-C^{16}), 3.04 (t, 2H, *J* = 5.4 Hz, H-C^{23}), 3.11 (s, 3H, H-C^{26}), 4.07 (br, H, H-N^8), 4.18 (m, H, H-C^{17}), 5.18 (br, H, H-N^{20}), 7.16 (d, 2H, *J* = 8 Hz, H-C^{12}, H-C^{14}), 7.29 (d, 2H, *J* = 8 Hz, H-C^{11}, H-C^{15}).

Methyl 2-((tert-butoxycarbonyl)amino)-3-(4-((4-chloro-6- morpholino-1,3,5-triazin-2-yl)oxy) phenyl)propanoate (**4e**)

Yield: 90%, white powder, MP:80 °C, IR (KBr, cm^{-1}) ν: 3356 (NH), 1714 (C=O), 1587 (C=N), 1532 (CC aromatic), 1364 (C-N), 1249 (C-O), 795 (CCl). ^{1}H NMR (400 MHz, DMSO-d_6) δ: 1.33 (s, 9H, Boc), 2.76 (t, 4H, *J* = 3 Hz, H-C^{21}, H-C^{25}), 2.87(d, 2H, *J* = 4 Hz, H-C^{16}), 3.61 (s, 3H, H-C^{27}), 3.73 (t, 4H, *J* = 3 Hz, H-C^{22}, H-C^{24}), 4.22 (m, H, H-C^{17}), 4.95 (br, H, H-N^{20}), 7.15 (d, 2H, *J* = 7 Hz, H-C^{12}, H-C^{14}), 7.32 (d, 2H, *J* = 7 Hz, H-C^{11}, H-C^{15}).

Methyl 2-((tert-butoxycarbonyl)amino) -3-(4-((4-chloro-6-(hexylamino) -1,3,5-triazin-2-yl)oxy) phenyl)propanoate (**4f**)

Yield: 85%, white powder, MP: 87 °C, IR (KBr, cm^{-1}) ν: 3318 (NH), 2962(CH aliphatic), 1720 (C=O), 1586 (C=N), 1509 (CC aromatic), 1293 (C-N), 1197 (C-O), 870 (CCl). ^{1}H NMR (400 MHz, DMSO-d_6) δ: 0.84 (t, 3H, *J* = 3 Hz, H-C^{26}), 1.19 (m, 8H, H-C^{22}, H-C^{23}, H-C^{24}, H-C^{25}), 1.39 (s, 9H, Boc), 2.84 (d, 2H, *J* = 3 Hz, H-C^{16}), 3.05 (q, 2H, *J* = 4 Hz, H-C^{21}), 3.61 (s, 3H, H-C^{28}), 3.83 (br, H, H-N^8), 4.18 (m, H, H-C^{17}), 5.2 (br, H, H-N^{20}), 7.15 (d, 2H, *J* = 8 Hz, H-C^{12}, H-C^{14}), 7.31 (d, 2H, *J* = 8 Hz, H-C^{11}, H-C^{15}).

2-amino-3-(4-((4-chloro-6-(propylamino)-1,3,5-triazin-2-yl)oxy)phenyl)propanoic acid (**5a**)

Yield: 65%, white powder, MP: 160 °C, IR (KBr, cm^{-1}) ν: 2976 (CH aliphatic), 2593-3300 (OH), 1737 (C=O), 1619 (C=N), 1519 (CC aromatic), 1221 (C-O), 717 (CCl). ^{1}H NMR (400 MHz, DMSO-d_6) δ: 0.85 (t, 3H, *J* = 4Hz, H-C^{24}), 1.43 (m, 2H, H-C^{23}), 2.97 (d, 2H, *J* = 4 Hz, H-C^{16}), 3.23 (m, 2H, H-C^{22}), 3.68 (br, 2H, H-N^{21}), 4.05 (br, H, H-N^8), 4.11 (m, H, H-C^{17}), 6.72 (d, 2H, *J* = 7Hz H-C^{12}, H-C^{14}), 7.07 (d, 2H, *J* = 7 Hz, H-C^{11}, H-C^{15}), 11.19 (s, H, H-O^{19}).

2-amino-3-(4-((4-chloro-6-(ethylamino)-1,3,5-triazin-2-yl)oxy)phenyl)propanoic acid (**5b**)

Yield: 70%, white powder, MP: 170 °C, IR (KBr, cm^{-1}) ν: 3487 (NH), 2318-3165(OH), 1725 (C=O), 1613 (C=N), 1558 (CC aromatic), 1234 (C-O), 747(CCl). ^{1}H NMR (400 MHz, DMSO-d_6) δ: 1.07 (t, 3H, *J* = 3 Hz, H-C^{23}), 2.96 (d, 2H, *J* = 4 Hz, H-C^{16}), 3.07 (m, 2H, H-C^{22}), 3.24 (br, 2H, H-N^{21}), 3.69 (br, H, H-N^8), 4.13 (m H, H-C^{17}), 6.72 (d, 2H, *J* = 8 Hz, H-C^{12}, H-C^{14}), 7.17 (d, 2H, *J* = 8 Hz, H-C^{11}, H-C^{15}), 11.19 (s, H, H-O^{19}).

2-amino-3-(4-((4-(butylamino)-6-chloro-1,3,5-triazin-2-yl)oxy)phenyl)propanoic acid (**5c**)

Yield: 85%, white powder, MP: 150 °C, IR (KBr, cm^{-1}) ν: 3536 (NH), 2627-3400 (OH), 1719 (C=O), 1604 (CC aromatic), 1236 (C-O), 771 (CCl). ^{1}H NMR (400 MHz, DMSO-d_6) δ: 0.85 (t, 3H, *J* = 3 Hz, H-C^{25}), 1.25 (m, 2H, H-C^{21}), 1.33 (m, 2H, H-C^{22}), 2.93 (d, 2H, *J* = 4 Hz, H-C^{16}), 3.24 (m, 2H, H-C^{23}), 3.65 (br, 2H, H-N^{20}), 4.06 (br, H, H-N^8), 4.11 (m, H, H-C^{17}), 6.72 (d, 2H, *J* = 7 Hz, H-C^{12}, H-C^{14}), 7.07 (d, 2H, *J* = 7 Hz, H-C^{11}, H-C^{15}), 10.85 (s, H, H-O^{24}).

2-amino-3-(4-((4-chloro-6-(isobutylamino)-1,3,5-triazin-2-yl)oxy)phenyl)propanoic acid (**5d**)

Yield: 75%, white powder, MP: 150 °C, IR (KBr, cm^{-1}) ν: 3473 (NH), 2500-3500 (OH), 1743 (C=O), 1257 (C-O), 905 (CCl). ^{1}H NMR (400 MHz, DMSO-d_6) δ: 0.83 (d, 6H, *J* = 3.5 Hz, H-C^{21} , H-C^{24}), 1.73 (m, H, H-C^{22}), 3.01 (d, 2H, *J* = 3 Hz, H-C^{16}), 3.10 (q, 2H, *J* = 3 Hz, H-C^{23}), 3.67 (br, 2H, H-N^{20}), 3.70 (br, H, H-N^8), 4.04 (m, H, H-C^{17}), 6.71 (d, 2H, *J* = 7 Hz, H-C^{12}, H-C^{14}), 7.06 (d, 2H, *J* = 7 Hz, H-C^{11}, H-C^{15}), 10.96 (s, H, H-O^{25}).

2-amino-3-(4-((4-chloro-6-morpholino-1,3,5-triazin-2-yl)oxy)phenyl)propanoic acid (**5e**)

Yield: 60%, white powder, MP: 175 °C, IR (KBr, cm^{-1}) ν: 3404 (NH), 2508-3500 (OH), 1734 (C=O), 1557 (CC aromatic), 1260 (CN), 1212 (C-O), 814 (CCl). ^{1}H NMR (400 MHz, DMSO-d_6) δ: 2.60 (t, 4H, *J* = 3 Hz, H-C^{21}, H-C^{25}), 3.10 (d, 2H, *J* = 3 Hz, H-C^{16}), 3.57 (t, 4H, *J* = 3 Hz, H-C^{22}, H-C^{24}), 3.87 (br, 2H, N^{20}), 4.17 (q, H, *J* = 3 Hz, H-C^{17}), 6.72 (d, 2H, *J* = 8 Hz, H-C^{12}, H-C^{14}), 7.07 (d, 2H, *J* = 8 Hz, H-C^{11}, H-C^{15}), 10.62 (s, H, H-O^{26}).

2-amino-3-(4-((4-chloro-6-(hexylamino)-1,3,5-triazin-2-yl)oxy)phenyl)propanoic acid (**5f**)

Yield: 65%, white powder, MP: 165 °C, IR (KBr, cm^{-1}) ν: 3020(CH aromatic), 2304-3500 (OH), 1724 (C=O), 1620 (C=N), 1518 (CC aromatic), 1211 (C-O), 809 (CCl). ^{1}H NMR (400 MHz, DMSO-d_6) δ: 0.85 (t, 3H, *J* = 3 Hz, H-C^{27}), 1.13-1-34 (m, 8H, H-C^{25}, H-C^{24}, H-C^{23}, H-C^{22}), 2.94 (d, 2H, *J* = 3 Hz, H-C^{16}), 3.34(q, 2H, *J* = 3 Hz, H-C^{21}), 3.41 (br, 2H, H-N^{20}), 3.91(br, H, H-N^8), 4.30 (q, H, *J* = 3 Hz, H-C^{17}), 7.22 (d, 2H, *J* = 8 Hz, H-C^{12}, H-C^{14}), 7.33 (d, 2H, *J* = 8 Hz, H-C^{11}, H-C^{15}), 11.02 (s, H, H-O^{26}).

In vivo study

As mentioned above, the compounds **5a-5f** were injected at 0.3, 1, and 3 mg/kg doses. Each group contained six male Wistar rats (180-200 mg). Lymphocyte percentage diagrams are illustrated in Fig. 1.

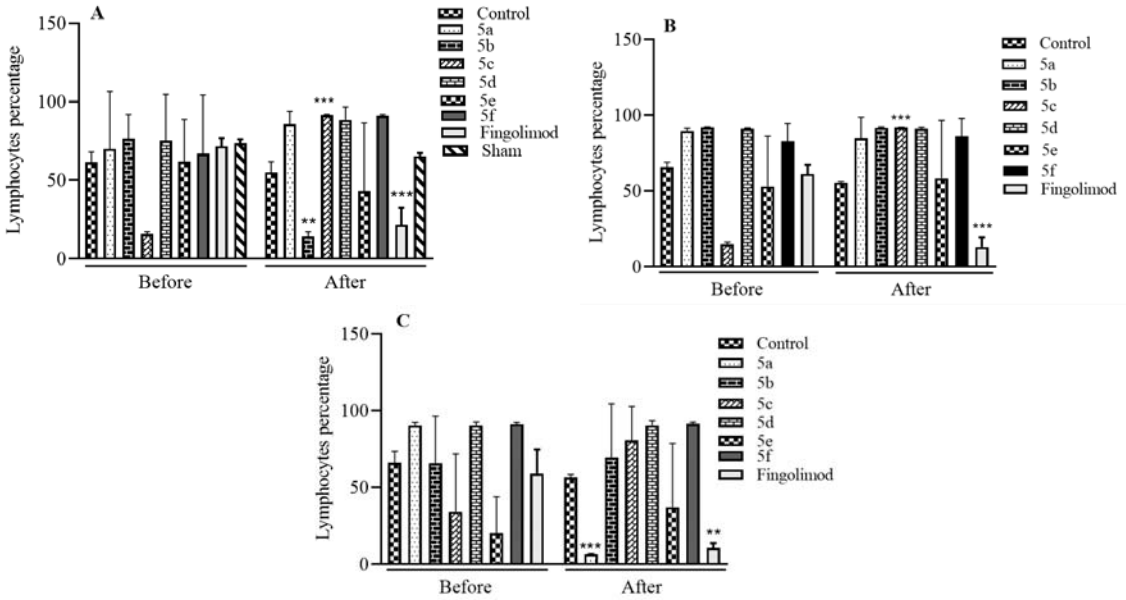

Fig. 1. Lymphocytes percentage before and after the injection of **5a-5f** and fingolimod at (A) 0.3 mg/kg, (B) 1 mg/kg, and (C) 3 mg/kg. Lymphocyte percentage was determined using the flow cytometry method. Data are shown as mean ± SD. $^{**}P < 0.01$ and $^{***}P < 0.001$ indicate significant differences before and after injection of the same compound.

DISCUSSION

The binding of novel synthesized triazine-tyrosine hybrid compounds (**5a-5f**) to S1P1R was investigated with a docking procedure. Fingolimod was used as a reference and according to the docking results; the novel designed compounds could be fitted well within the binding site cavity of the S1P1R, showing acceptable ΔG values (Table 1). The docking results demonstrated that the amino group of all compounds, except **5b**, interacts electrostatically with GLU 321 residue, mimicking the amino group of fingolimod. Triazine ring has a role in π-π interactions with TYR 306 and TRP 299 residues in **5a**, **5b**, and **5d** similar to the benzene ring of fingolimod. In compound **5c**, the triazine ring interacts hydrophobically with MET 243 and VAL211. N-alkyl substitute acts like the aliphatic chain of fingolimod and is responsible for the hydrophobic interactions with TYR306, Met243, PHE288, and TRP299. The N-morpholine substituted compound, **5e**, has the best free energy of binding. In this compound similar to fingolimod, **5a**, **5b**, and **5d**, the amino group interacts electrostatically with GLU 321 residue and the morpholine ring interacts hydrophobically with key residues, PHE 288 and TRP 299. The interactions of fingolimod, **5a,** and **5b,** as representative structures, with binding residues of the S1P1R, are shown in Fig. 2. As shown in Table 1, ΔG binding of the suggested derivatives was as follows; **5e** > **5d** > **5f** > **5a** > **5c** > **5b** > fingolimod.

In the present work, six triazine-tyrosine compounds **5a-5f** were synthesized according to the procedure shown in Scheme 2. Since one site of triazine can be substituted at low temperature, in the first step, different amines **a-f** was reacted with cyanuric chloride at low temperature (0-5 °C). Both melting point and the IR spectrum of **2a-2f** were according to the reported values in the literature (24-27).

The disubstituted s-triazine compounds (**4a-4f**) were obtained by the reaction of **2a-2f** with N-Boc-tyr-OMe ester. In IR spectra of these compounds, the peaks around 1730 cm^{-1} confirm the presence of esteric C=O groups in their framework. After de-protection of the tyrosine moiety by HCl, an acidic C=O group was observed around 1710 cm^{-1} which confirmed the conversion of ester to an acid group. Additionally, a new band, observed at 2500-3500 cm^{-1} was assigned to the vibration of a hydroxyl group of acid in the IR spectrum, confirming the formation of the deprotected final products. The ^{1}H-NMR spectral data of the intermediates and final products recorded in DMSO-d6 along with their assignments were reported in the experimental part. All the aromatic and aliphatic H-atoms were found in their expected region. The peaks around 0.8-3.7 ppm are attributable to the aliphatic H-atoms of these compounds. The NH of these intermediates exhibited a broad singlet around 4-5 ppm. Also, four aromatic hydrogens of the tyrosine ring were observed around 7-8 ppm. Finally, observation of a peak around 11 ppm and also the absence of a peak related to the tert-butoxy group around 1 ppm confirmed the structure of the final synthesized compounds.

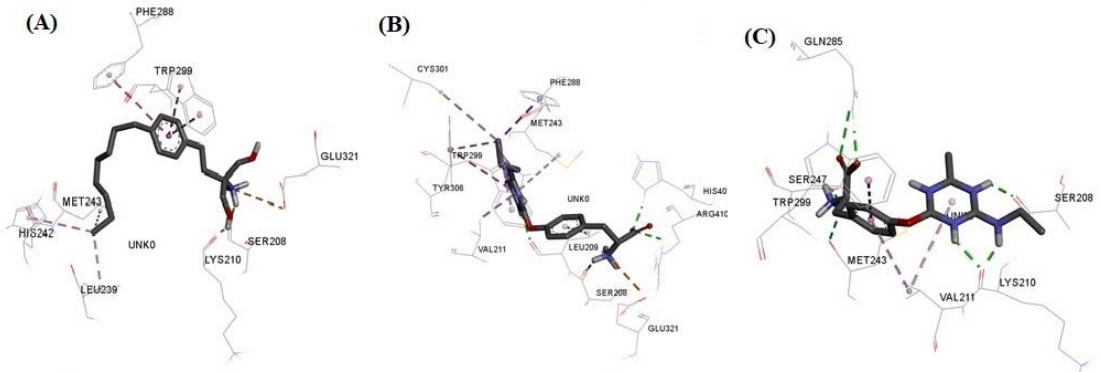

Fig. 2. Graphical representation of (A) fingolimod, (B) **5a,** and (C) **5b** interactions with binding residues of the sphingosine-1-phosphate receptor.

According to the *in vivo* results of this project, fingolimod at 0.3, 1, and 3 mg/kg has reducing effects on the percentage of the lymphocytes i.e., dose 0.3 mg/kg from 71.5% to 21.5%, dose 1 mg/kg from 61.2% to 12.9%, and dose 3 mg/kg from 58.8% to 10.6%, before and after treatment, respectively. These results are in accordance with the studies conducted by Skidmore *et al* (29). Studies have shown that the ability of fingolimod to reduce the number of lymphocytes is due to its interaction with the S1P1R subunit (30,31).

The results of our experiments demonstrated that compound **5a**, with propylamine substitution, at 3 mg/kg, has an acceptable activity and reduced the average percentage of lymphocytes from 90.4% to 6.9%. Ethylamine substitution on compound **5b** at 0.3 mg/kg, resulted in a significant reduction of lymphocytes from 76.3% to 14.0%. Interestingly, both **5a** and **5b** compounds have short-chain substitutions. Additionally, compound **5c** with butylamine substitution, significantly increased the percentage of lymphocytes at 3 and 0.3 mg/kg while it was expected to be more effective due to the lipophilicity of the butyl amine chain. Other compounds such as **5e** with morpholine, **5f** with hexylamine, and **5d** with isobutyl amine substitution did not show a significant effect on lymphocyte number. In addition, the reports obtained from the control and sham groups showed that the effects of the carrier and injection are negligible and have not caused any problems in the study process.

In this study the modification was carried out on the three dominant segments of the representative S1P1 modulator, fingolimod; modification of the polar-head group, replacement of the triazine as a linker and different aliphatic amine moieties as the hydrophobic tail. The insertion of moieties possessing both amine and carboxyl functional groups as the polar head of the structure of S1P1 modulators, linearly or cyclically, has shown good effects (32,33). To the best of our knowledge, the simultaneous use of tyrosine amino acid as polar head and triazine as a linker has not been reported in the design of S1P1 modulators. Similar to earlier studies reported on different hybrid structures, the results of this study showed a dose-dependent lymphocyte depletion manner (29,34,35). But unlike others (36,37), compounds possessing larger hydrophobic tails showed weaker effects while compounds with smaller hydrophobic groups, such as ethyl and propyl, exhibited better effects on lymphocyte depletion which may be due to the large size of the total structure of these new compounds, perhaps less entry into the receptor site. Therefore, only two compounds **5a** and **5b** are suggested for future studies.

CONCLUSION

In this study, a series of novel hybrid derivatives bearing s-triazine and tyrosine moieties were designed and synthesized as an S1P1 modulator. According to the structural requirements of S1P1 modulators, these compounds contain tyrosine as a polar-head group, triazine moiety as a linker, and aliphatic amine as a lipophilic tail. The docking study of the designed compounds with S1P1 as a key receptor in MS treatment revealed that these compounds could be fitted well in the receptor active site through electrostatic, π-π, and hydrophobic interactions. Structures of the new compounds were characterized by ^{1}H NMR and IR spectra. The results of lymphocyte count revealed that compounds **5a** and **5b** with propyl and ethyl substitutes showed the maximum activity *in vivo* and other compounds with longer alkyl and also morpholine substitutions did not show good activity. These results were fair in terms of a triggering point for further research on the triazine-tyrosine hybrid, but it appears that better candidates must be developed and evaluated more accurately *in vivo*.

Acknowledgments

This project was financially supported by the Vice Chancellery of Research of Isfahan University of Medical Sciences, Isfahan, I.R. Iran under Grant No. 298018

Conflicts of interest statement

All authors declared no conflict of interest in this study.

Authors' contribution

G.A. Khodarahmi conceived and supervised the project; S. Saeidi performed the experiments, analyzed and interpreted the data; P. Asadi assisted in the docking study, synthesis of compounds, and writing the manuscript, M. Aliomrani advised the biological study of compounds; F. Hassanzadeh helped in the synthesis of compounds and interpretation of the spectra. The final version of the manuscript was approved by all authors.

REFERENCES

1. Banisharif-Dehkordi F, Mobini-Dehkordi M, Shakhsi-Niaei M, Mahnam K. Design and molecular dynamic simulation of a new double-epitope tolerogenic protein as a potential vaccine for multiple sclerosis disease. Res Pharm Sci. 2019;14(1):20-26. DOI: 10.4103/1735-5362.251849.
2. Mitra NK, Xuan KY, Teo CC, Xian-Zhuang N, Singh A, Chellian J. Evaluation of neuroprotective effects of alpha-tocopherol in cuprizone-induced demyelination model of multiple sclerosis. Res Pharm Sci. 2020;15(6):602-611. DOI: 10.4103/1735-5362.301345.
3. Yahyazadeh S, Esmaeil N, Shaygannejad V, Mirmosayyeb O. Comparison of follicular T helper cells, monocytes, and T cells priming between newly diagnosed and rituximab-treated MS patients and healthy controls. Res Pharm Sci. 2022;17(3):315-323. DOI: 10.4103/1735-5362.343085.
4. Weinshenker BG. Epidemiology of multiple sclerosis. Neurol Clin. 1996;14(2):291-308. Doi: 10.1016/SO733-8619(05)70257-7.
5. Bordet R, Camu W, De Seze J, Laplaud D-A, Ouallet J-C, Thouvenot E. Mechanism of action of s1p receptor modulators in multiple sclerosis: the double requirement. Rev Neurol(Paris). 2020;176(1-2):100-112. DOI: 10.1016/j.neurol.2019.02.007.
6. Pyne NJ, Tonelli F, Lim KG, Long J, Edwards J, Pyne S. Targeting sphingosine kinase 1 in cancer. Adv Biol Regul. 2012;52(1):31-38. DOI: 10.1016/j.advenzreg.2011.07.001.
7. Vickers NJ. Animal communication: when i'm calling you, will you answer too? Curr Biol. 2017;27(14):R713-R715. DOI: 10.1016/j.cub.2017.05.064.
8. Pyne NJ, Pyne S. Sphingosine 1-phosphate receptor 1 signaling in mammalian cells. Molecules. 2017;22(3):344,1-18. DOI: 10.3390/molecules22030344.
9. Pyne S, Adams DR, Pyne NJ. Sphingosine 1-phosphate and sphingosine kinases in health and disease. Prog Lipid Res, 2016; 62:93-106. DOI: 10.1016/j.plipres.2016.03.001.
10. O'Sullivan C, Dev KK. The structure and function of the S1P1 receptor. Trends Pharmacol Sci. 2013;34(7):401-412. DOI: 10.1016/j.tips.2013.05.002.
11. Mitra NK, Singh NSG, Wadingasafi NANB, Chellian J. Locomotor and histological changes in a cuprizone-induced animal model of multiple sclerosis: comparison between alpha-tocopherol and fingolimod. Res Pharm Sci. 2022;17(2):134-142. DOI: 10.4103/1735-5362.335172.
12. Brinkmann V, Billich A, Baumruker T, Heining P, Schmouder R, Francis G, *et al*. Fingolimod (FTY720): discovery and development of an oral drug to treat multiple sclerosis. Nat Rev Drug Discov. 2010;9(11):883-897. DOI: 10.1038/nrd3248.
13. Chun J, Hartung H-P. Mechanism of action of oral fingolimod (FTY720) in multiple sclerosis. Clin Neuropharmacol. 2010;33(2):91-101. DOI: 10.1097/WNF.0b013e3181cbf825.
14. Dev KK, Mullershausen F, Mattes H, Kuhn RR, Bilbe G, Hoyer D, *et al.* Brain sphingosine-1-phosphate receptors: implication for FTY720 in the treatment of multiple sclerosis. Pharmacol Ther. 2008;117(1):77-93. DOI: 10.1016/j.pharmthera.2007.08.005.
15. Hu J, Zhao M, Mi J, Wang B, Sheng L, Chen H, *et al*. Insights into the metabolic characteristics of aminopropanediol analogues of SYLs as S1P1 modulators: from structure to metabolism to druggability. 18th World Congress of Basic and Clinical Pharmacology. Proceedings for annual meeting of the Japanese pharmacological society. 2018;WCP2018.0:PO2-14-27. DOI: 10.1254/jpssuppl.wcp2018.0_po2-14-27.
16. Dyckman AJ. Modulators of sphingosine-1-phosphate pathway biology: recent advances of sphingosine-1-phosphate receptor 1 (S1P1) agonists and future perspectives. J Med Chem. 2017;60(13):5267-5289. DOI: 10.1021/acs.jmedchem.6b01575.
17. Saha AK, Yu X, Lin J, Lobera M, Sharadendu A, Chereku S, *et al.* Benzofuran derivatives as potent, orally active S1P1 receptor agonists: a preclinical lead molecule for MS. ACS Med Chem lett. 2011;2(2):97-101. DOI: 10.1021/ml100227q.
18. Li Z, Chen W, Hale JJ, Lynch CL, Mills SG, Hajdu R, *et al*. Discovery of potent 3, 5-diphenyl-1, 2, 4-oxadiazole sphingosine-1-phosphate-1 (S1P1) receptor agonists with exceptional selectivity against S1P2 and S1P3. J Med Chem. 2005;48(20):6169-6173. DOI: 10.1021/jm0503244.
19. Guan B, Zhang C, Ning J. EDGA: a population evolution direction-guided genetic algorithm for protein-ligand docking. J Comput Biol. 2016;23(7):585-596. DOI: 10.1089/cmb.2015.0190.
20. BIOVIA DS, Discovery Studio Visualizer, 4.5, San Diego: Dassault Systèmes, 2021.

21. Froimowitz M. HyperChem: a software package for computational chemistry and molecular modeling. Biotechniques. 1993;14(6):1010-1013. PMID: 8333944.
22. Eberhardt J, Santos-Martins D, Tillack A, Forli S. AutoDock Vina 1.2. 0: new docking methods, expanded force field, and Python bindings. J Chem Inf Model. 2021;61(8):3891-3898. DOI: 10.1021/acs.jcim.1c00203.
23. Trott O, Olson AJ. AutoDock Vina: improving the speed and accuracy of docking with a new scoring function, efficient optimization, and multithreading. J Comput Chem. 2010;31(2):455-461. DOI: 10.1002/jcc.21334.
24. The PyMOL Molecular graphics system, Version 1.2r3pre, Schrödinger, LLC.
25. Mannion JC, Dax SL, Golder FG, Macintyre DE, Mcleod J, Ozola V, *et al*, inventors; Novel orally bioavailable breathing control modulating compounds, and methods of using same. US Patent CA2891342A1, 2014.
26. Manohar S, Khan SI, Rawat DS. Synthesis of 4-aminoquinoline-1, 2, 3-triazole and 4-aminoquinoline-1, 2, 3-triazole-1, 3, 5-triazine hybrids as potential antimalarial agents. Chem Biol Drug Des. 2011;78(1):124-136. DOI: 10.1111/j.1747-0285.2011.01115.x.
27. Beran GJO. Porous materials: designed and then realized. Nat Mater. 2017;16(6):602-604. DOI: 10.1038/nmat4913.
28. Fujii S, Kobayashi T, Nakatsu A, Miyazawa H, Kagechika H. Synthesis and structure-activity relationship study of triazine-based inhibitors of the DNA binding of NF-κB. Chem Pharm Bull(Tokyo). 2014;62(7):700-708. DOI: 10.1248/cpb.c14-00218.
29. Skidmore J, Heer J, Johnson CN, Norton D, Redshaw S, Sweeting J*, et al*. Optimization of sphingosine-1-phosphate-1 receptor agonists: effects of acidic, basic, and zwitterionic chemotypes on pharmacokinetic and pharmacodynamic profiles. J Med Chem. 2014;57(24):10424-10442. DOI: 10.1021/jm5010336.
30. Bajrami A, Pitteri M, Castellaro M, Pizzini F, Romualdi C, Montemezzi S*, et al.* The effect of fingolimod on focal and diffuse grey matter damage in active MS patients. J Neurol. 2018;265(9):2154-2161. DOI: 10.1007/s00415-018-8952-2.
31. Van Doorn R, Van Horssen J, Verzijl D, Witte M, Ronken E, Van Het Hof B *et al*. Sphingosine 1-phosphate receptor 1 and 3 are upregulated in multiple sclerosis lesions. Glia. 2010;58(12):1465-1476. DOI: 10.1002/glia.21021.
32. Bolli MH., Lescop C, and Nayler O. Synthetic sphingosine 1-phosphate receptor modulators-opportunities and potential pitfalls. Curr Top Med Chem, 2011;11(6):726-757. DOI: 10.2174/1568026611109060726.
33. Roberts, E, Guerrero M, Urbano M, Rosen H. Sphingosine 1-phosphate receptor agonists: a patent review (2010-2012). Expert Opin Ther Pat. 2013;23(7):817-841. DOI: 10.1517/13543776.2013.783022.
34. Cee VJ, Frohn M, Lanman BA, Golden J, Muller K, Neira S, *et al.* Discovery of AMG 369, a thiazolo [5, 4-b] pyridine Agonist of S1P1 and S1P5. ACS Med Chem Lett. 2011;2(2):107-112. DOI: 10.1021/ml100306h.
35. Nishi T, Miyazaki S, Takemoto T, Suzuki K, Iio Y, Nakajima K*, et al*. Discovery of CS-0777: a potent, selective, and orally active S1P1 agonist. ACS Med Chem Lett. 2011;2(5):368-372. DOI: 10.1021/ml100301k.
36. Saha AK, Yu X, Lin J, Lobera M, Sharadendu A, Chereku S, *et al*. Benzofuran derivatives as potent, orally active S1P1 receptor agonists: a preclinical lead molecule for MS. ACS Med Chem Lett. 2011;2(2):97-101. DOI: 10.1021/ml100227q.
37. Bolli MH, Abele S, Birker M, Bravo R, Bur D, de Kanter R, *et al*. Novel S1P1 receptor agonists-part 3: from thiophenes to pyridines. J Med Chem. 2014;57(1):110-130. DOI: 10.1021/jm4014696.